



Sensitivity of a model projection of near-surface permafrost degradation to soil column depth and representation of soil organic matter

David M. Lawrence,¹ Andrew G. Slater,² Vladimir E. Romanovsky,³ and Dmitry I. Nicolsky³

Received 31 July 2007; revised 16 January 2008; accepted 21 February 2008; published 6 May 2008.

[1] The sensitivity of a global land-surface model projection of near-surface permafrost degradation is assessed with respect to explicit accounting of the thermal and hydrologic properties of soil organic matter and to a deepening of the soil column from 3.5 to 50 or more m. Together these modifications result in substantial improvements in the simulation of near-surface soil temperature in the Community Land Model (CLM). When forced off-line with archived data from a fully coupled Community Climate System Model (CCSM3) simulation of 20th century climate, the revised version of CLM produces a near-surface permafrost extent of $10.7 \times 10^6 \text{ km}^2$ (north of 45°N). This extent represents an improvement over the $8.5 \times 10^6 \text{ km}^2$ simulated in the standard model and compares reasonably with observed estimates for continuous and discontinuous permafrost area ($11.2\text{--}13.5 \times 10^6 \text{ km}^2$). The total extent in the new model remains lower than observed because of biases in CCSM3 air temperature and/or snow depth. The rate of near-surface permafrost degradation, in response to strong simulated Arctic warming ($\sim +7.5^\circ\text{C}$ over Arctic land from 1900 to 2100, A1B greenhouse gas emissions scenario), is slower in the improved version of CLM, particularly during the early 21st century (81,000 versus $111,000 \text{ km}^2 \text{ a}^{-1}$, where a is years). Even at the depressed rate, however, the warming is enough to drive near-surface permafrost extent sharply down by 2100. Experiments with a deep soil column exhibit a larger increase in ground heat flux than those without because of stronger near-surface vertical soil temperature gradients. This appears to lessen the sensitivity of soil temperature change to model soil depth.

Citation: Lawrence, D. M., A. G. Slater, V. E. Romanovsky, and D. I. Nicolsky (2008), Sensitivity of a model projection of near-surface permafrost degradation to soil column depth and representation of soil organic matter, *J. Geophys. Res.*, 113, F02011, doi:10.1029/2007JF000883.

1. Introduction

[2] The fate of permafrost is an important question for climate change science given model projections that indicate that steadily rising greenhouse gas concentrations in the atmosphere may drive a rapid and considerable rise in Arctic land temperatures during the 21st century [Chapman and Walsh, 2007]. Of particular concern is what may happen to permafrost that is currently found in near-surface soils as this portion is most vulnerable to climate change and its degradation has the potential to initiate a number of feedbacks, predominantly positive, in the Arctic and global climate system [McGuire et al., 2006].

[3] Permafrost degradation and rising soil temperatures are at the heart of many of these potential feedbacks. With

recent observations indicating that soil temperatures are rising, in some cases quite rapidly [Osterkamp and Romanovsky, 1999; Romanovsky et al., 2002; Osterkamp, 2005], and that near-surface permafrost is degrading in many locations [Payette et al., 2004; Jorgenson et al., 2006; Osterkamp and Jorgenson, 2006], a better understanding of these feedbacks and their possible implications for future climate are urgently required. Permafrost thaw alters soil structural and hydrologic properties, with impacts ranging from changes in the spatial extent of lakes and wetlands [Smith et al., 2005], freshwater fluxes to the Arctic ocean, ecosystem functioning [Payette et al., 2004], to the partitioning of surface energy. Warming of the soil may also enhance decomposition of soil organic matter which could conceivably lead to the release of vast quantities of carbon dioxide to the atmosphere [Zimov et al., 2006]. If soils become wetter, the production of methane from saturated soils, wetlands, and lakes could also increase [Christensen et al., 2004; Zimov et al., 2006]. Warmer soil temperatures also tend to increase microbial activity, liberating nitrogen, which in nutrient-limited Arctic ecosystems may prompt shrub growth [Sturm et al., 2001; Sturm et al., 2005; Tape

¹Climate and Global Dynamics Division, National Center for Atmospheric Research, Boulder, Colorado, USA.

²Cooperative Institute for Research in Environmental Sciences, University of Colorado, Boulder, Colorado, USA.

³Geophysical Institute, University of Alaska Fairbanks, Fairbanks, Alaska, LISA.

et al., 2006]. Expansion of shrub cover has its own positive feedback on climate because of the lower albedo of shrubs compared to tundra and because areas with shrubs have a lower snow albedo, and consequently earlier snowmelt than snow covered tundra [Chapin *et al.*, 2005]. The scientific challenge is to increase our understanding of these complex interactions and, on the basis of this improved understanding, to improve the fidelity of model predictions of future Arctic and global environment and climate.

[4] Coupled global climate models (GCMs) are advancing to the point that many of the aforementioned biogeophysical, biogeochemical, and hydrological interactions and feedbacks, of which many are directly or indirectly related to permafrost degradation, are or will soon be captured. Here, we describe and analyze improvements in the depiction of permafrost in the Community Land Model (CLM). CLM is the global land-surface scheme that is included in the Community Climate System Model (CCSM). The improvements to CLM represent another step toward a more complete depiction of the integrated Arctic processes in a global modeling system.

[5] Lawrence and Slater [2005] presented data from a coupled GCM indicating that the extent of near-surface permafrost may contract substantially during the 21st century as Arctic temperatures soar. The extent of near-surface permafrost metric is defined in that paper as the globally integrated area of grid boxes that contain at least one soil layer in the top 3.5 m of soil that remains frozen for 24 or more consecutive months. Burn and Nelson [2006] and Delisle [2007] argue that such a significant change in near-surface permafrost extent is not likely to occur and that the results presented by Lawrence and Slater [2005] overestimate the extent of permafrost degradation because of deficiencies in the land model. Nicolsky *et al.* [2007], Alexeev *et al.* [2007], and Stevens *et al.* [2007] show that correcting some common simplifications in GCM land surface schemes can improve the simulation of soil temperatures across seasonal, decadal, and century timescales. The suggested improvements include a significant deepening of the soil column to account for the thermal inertia provided by the cold deep permafrost layers and the explicit treatment of the insulating properties of soil organic matter. Organic-rich soils are prevalent throughout much of the Arctic.

[6] In this paper, we examine the sensitivity of near-surface permafrost degradation projections with the CLM to the incorporation of a deeper soil column and inclusion of the physical properties of soil organic matter. In section 2, we introduce CLM, describe the organic soil [Lawrence and Slater, 2007] and deep soil model configurations, and outline the experimental design. In section 3, we assess the sensitivity of climate-change-induced soil temperature and large-scale near-surface permafrost degradation to soil depth and organic soil. A discussion of the implications of these results as well as a review of other sources of uncertainty in projections of permafrost degradation is provided in section 4, followed by a summary in section 5.

2. Model and Forcing Data Set Descriptions

2.1. CLM

[7] The Community Land Model (CLM3, for a detailed technical description see Oleson *et al.* [2004]) can be run in

both off-line mode or as component of the Community Climate System Model (CCSM3 [Collins *et al.*, 2006]). The land surface is represented by fractional coverage of lakes, wetland, bare soil, glacier, and up to four plant functional types (PFT) for each grid box. The fractional coverage, of each surface type as well as monthly leaf and stem area indices for each PFT is derived from Moderate Resolution Imaging Spectroradiometer (MODIS) land surface product [Lawrence and Chase, 2007]. CLM3 represents conductive heat transfer in soil and snow, canopy, soil, and snow hydrology, as well as stomatal physiology and photosynthesis. Fluxes of energy and moisture are modeled independently for each surface type and aggregated before being passed to the atmosphere model. CLM3 includes a 5-layer snow model which simulates processes such as accumulation, melt, compaction, snow aging, and water transfer across layers. The standard soil column has 10 layers with exponentially deeper nodal depths, z , (m),

$$z_i = f_s \{ \exp[0.5(i - 0.5)] - 1 \},$$

where $f_s = 0.025$ is a scaling factor. The thickness of each layer, Δz , (m), is

$$\Delta z_i = \begin{cases} 0.5(z_1 + z_2) & i = 1 \\ 0.5(z_{i+1} - z_{i-1}) & i = 2, 3, \dots, N-1 \\ z_N - z_{N-1} & i = N \end{cases},$$

where $N = 10$ is the number of soil layers. The depths at the layer interfaces, $z_{h,i}$ (m) are

$$z_{h,i} = \begin{cases} 0.5(z_1 + z_{i+1}) & i = 1, 2, \dots, N-1 \\ z_N + 0.5\Delta z_N & i = N \end{cases}.$$

The total column depth is 3.43 m

[8] Heat conduction in the soil is determined by numerically solving the second law of heat conduction equation, which in one-dimensional form is

$$c \frac{\partial T}{\partial t} = \frac{\partial}{\partial z} \left[\lambda \frac{\partial T}{\partial z} \right],$$

where c is the heat volumetric heat capacity ($\text{J m}^{-3} \text{K}^{-1}$), λ is the thermal conductivity ($\text{W m}^{-1} \text{K}^{-1}$), T is temperature, and t is time. The thermal and hydrologic properties of each soil layer are functions of soil liquid and ice water content, soil texture, and soil temperature. Soil texture, e.g., the sand and clay content for each layer for each grid point, is derived from the International Geosphere-Biosphere Programme soil data set [Global Soil Data Task, 2000]. The boundary conditions for the solution are the heat flux into the soil/snow at the top and zero heat flux at the bottom of the soil column. After the heat conduction equation is solved, soil temperatures are evaluated to determine if phase change should take place. If the new soil temperatures indicate that phase change has taken place, the excess or deficit of energy is determined and then used to melt or freeze the soil water and the temperatures are adjusted back to the freezing level. Checks are made to ensure that if the excess or deficit of energy exceeds that which is required to complete the phase change of that soil layer's water, then

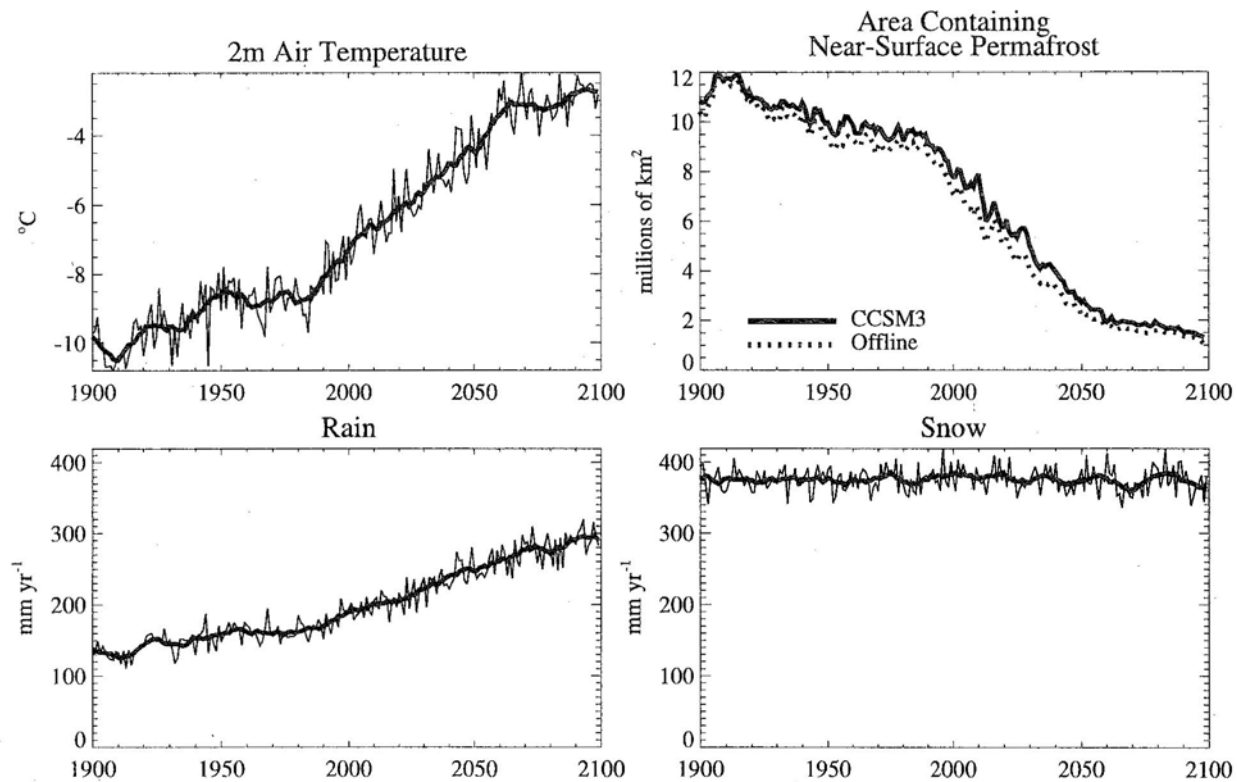


Figure 1. Time series of 2 m air temperature, rain, and snow averaged over all nonice sheet Arctic land points (60–80°N). Thin lines are annual mean values, and thick lines are 11-year running average. Also shown is near-surface permafrost extent poleward of 45°N diagnosed from the fully coupled simulation (CCSM3) and from an off-line land-only simulation forced with 6-hourly data from the coupled simulation (off-line).

this excess energy goes toward heating or cooling the soil layer. Such a predictor-corrector method is reasonable for the model's standard 30-min time step. The hydrology scheme includes parameterizations for processes such as interception, throughfall, canopy drip, infiltration, surface runoff, subsurface drainage and redistribution of soil water within the soil column. Heat advection associated with water infiltrating into and through the soil is not considered.

2.2. Off-Line Transient Climate-Change-Forcing Data Set

[9] We assess the sensitivity of climate change-induced near-surface permafrost degradation to the inclusion of soil organic matter and a deeper soil column by forcing CLM off-line with atmospheric data obtained from a single ensemble member of the fully coupled transient 20th and 21st century climate-change integration conducted in support of the Intergovernmental Panel on Climate Change Fourth Assessment Report (IPCC AR4). The original CCSM3 20th century simulation was forced with observed natural and anthropogenic forcings (greenhouse gases, sulfate aerosols, volcanoes, ozone, solar variability, halocarbons, and black carbon aerosols), whereas the 21st century simulation was forced with the midrange SRES A1B emission scenario [Meehl *et al.*, 2006]. These simulations were conducted at T85 resolution (~1.4° latitude × 1.4° longitude). A full set of forcing data for the land model

(precipitation, temperature, downward solar and longwave radiation, surface wind speed, specific humidity, and air pressure) was archived every 6 h from this coupled simulation. This 6-hourly data was then interpolated to 30 min for the off-line simulations. For all experiments with the standard shallow CLM soil column, the model is spun-up for 200 years with year 1900 data. For the experiments with a deep soil column, the simulations are spun-up for an additional 200 years to account for the longer spin-up timescale of the deep soil layers. Soil temperature trends at all soil levels and for all model configurations are below 0.005°C a⁻¹, where a is years, by the end of the spin-up phase.

[10] Annual mean air temperature and precipitation trends from the coupled simulation, averaged over the Arctic land area (60–80°N), are shown in Figure 1. Arctic land air temperature rises by roughly +2°C from 1900 to 2000 and by a further +5.5°C by the year 2100. The Arctic also gets considerably wetter with total annual precipitation rising by ~30% over the course of the simulation.

[11] Also shown in Figure 1 is the diagnosed area, poleward of 45°N that contains near-surface permafrost in the model. Near-surface permafrost extent is defined, as shown by Lawrence and Slater [2005], as the integrated area where monthly mean soil temperature in at least one soil level remains below 0°C for 24 consecutive months. The diagnosed near-surface permafrost extent differs by

roughly 0.3 to $0.5 \times 10^6 \text{ km}^2$ ($\sim 5\%$ during 20th century) between the fully coupled simulation ($\text{CONTROL}_{\text{CCSM3}}$) and the off-line simulation with the same land-surface model but forced with 6-hourly data (interpolated to the standard 30-min time step) from the fully coupled simulation ($\text{CONTROL}_{\text{CLM3}}$). Soil temperature differences between these two simulations can be as large as 3°C for selected locations and months but soil temperatures in the two simulations tend to be fairly close to each other (65% of area within 0.5°C , 93% within 1.0°C). Soil water content also differs slightly across the two experiments (64% of area within 10% volumetric soil water content ($\text{mm}^3 \text{ mm}^{-3}$), 91% of area within 20%). The discrepancy in the simulated soil climate between the coupled and off-line simulations is due to a number of factors. The main one is that soil initial conditions in the fully coupled and off-line simulations differ. The land-surface state at year 1900 in the coupled simulation reflects the transient climate state at the end of a multicentury 1870 control integration followed by 30 years of simulation with specified natural and anthropogenic forcings (1870-1899), whereas the land-surface state in the off-line simulations is the product of multicentury spin-ups with repeat year 1900 forcing obtained from the coupled simulation. The soil climate differences may also reflect minor imperfections inherent in the experimental design which include the fact that the archived 6-hourly forcing data do not fully resolve the diurnal cycle and that two-way interactions between changes in atmospheric climate and changes in land surface state are not captured when the land model is run in off-line mode. These deficiencies are balanced by the vast computational cost savings between the fully coupled and off-line versions of the model and are considered acceptable for the purpose of this study, which focuses on the sensitivity of soil temperature change to land-surface model parameterizations in off-line simulations.

2.3. Modifications to CLM3

2.3.1. CLM3.5: Revised Hydrology

[12] The released version of CLM3 suffers from poor partitioning of evapotranspiration into its components (transpiration, soil evaporation, and canopy evaporation) and generally dry and unvarying deep soil moisture [Lawrence et al., 2007]. These deficiencies have largely been eliminated through a series of modifications to the released version, which includes a revised surface data set based on MODIS data [Lawrence and Chase, 2007], reductions in canopy interception [Lawrence et al., 2007] and incorporation of a two leaf model for photosynthesis [Thornton and Zimmerman, 2007], as well as a major reworking of the soil hydrology scheme [Niu et al., 2007]. Of direct relevance to this paper is the inclusion of a freezing point depression expression that permits liquid water to coexist with ice at temperatures below 0°C and enhances permeability into partially ice-filled soil [Niu and Yang, 2006]. Arctic soils tend to be closer to saturation in CLM3.5. Soil temperatures can differ by up to 2°C between CLM3 and CLM3.5 primarily because of changes in soil wetness but also because of differences in surface data sets. Since CLM3.5 is the new baseline version of CLM, we refer throughout the paper to simulations with this version of the model as

CONTROL, whereas simulations with the released version, CLM3, are referred to as $\text{CONTROL}_{\text{CLM3}}$.

2.3.2. Soil Organic Matter

[13] Molders and Rotmanovsky [2006] and Nicolsky et al. [2007] show that accounting for the physical properties of soil organic matter significantly improves soil temperature simulations. Lawrence and Slater [2007] describes how organic soil and its impact on soil thermal and hydraulic properties can be implemented into CLM. Briefly, a geographically distributed and profiled soil carbon density data set for CLM is derived by taking the soil carbon content obtained from the gridded *Global Soil Data Task* [2000] data set and distributing the carbon content for each grid box vertically through the CLM soil column according to some simple rules related to ecosystem type. A typical grid box with high organic soil content (e.g., $>40 \text{ kg m}^{-2}$) has an organic layer of roughly 5–30 cm depth which is underlain by a mixture of mineral and organic soil with the organic soil content decreasing sharply with depth. This data set is then used to adjust soil thermal and hydraulic parameters, on the basis of organic soil thermal and hydraulic properties obtained from the literature, to account for the organic matter present in any model soil layer. In off-line simulations with observed forcing, we see reductions in annual mean soil temperatures of up to 2.5°C when organic matter is included. Soil organic matter also influences soil hydrology. The greater porosity of organic soil leads to higher water contents, especially in the upper portion of the soil where the organic matter is concentrated. However, the high hydraulic conductivity of organic matter permits incident precipitation to quickly permeate through the topsoil layers, resulting in a comparatively dry surface layer and weaker soil evaporation. Simulations using this organic matter data set along with the revised parameterizations that account for the influence of soil carbon on the thermal and hydraulic properties of soil are referred to throughout the paper as SOILCARB . These modifications are added on top of the changes that make up CLM3.5.

2.3.3. Deep Soil

[14] Recent studies by Smerdon and Stieglitz [2006], Alexeev et al. [2007], and Stevens et al. [2007] have clearly demonstrated that the depth of the bottom boundary condition strongly influences seasonal and longer-timescale soil temperature dynamics. Soil depths of greater than 30m are preferred to reasonably simulate the annual cycle and decadal trends of subsurface temperatures. Even deeper soils may be preferable for longer-timescale forcing such as that associated with climate change. On the basis of the recommendations of these prior studies, we test CLM with soil depths ranging from 25 to 125 m. Deeper soil columns were obtained by adding from 4 to 7 exponentially thicker layers to the original 10 level soil model. For simplicity, the new layers are assumed to be hydrologically inactive, that is, water cannot pass into or out of these layers with hydrology calculations restricted to the upper 10 layers. The soil texture (% sand, % clay) from layer 10 of the original soil texture data set is used for all the additional layers and the deep soils are set to be wet ($\sim 90\%$ saturation).

[15] This representation of the deep ground is pragmatic. In reality, the deep ground should be fractured bedrock, with the depth to bedrock and type of bedrock varying geographically (although the depth to bedrock may actually be quite

Table 1. List of Experiment Names and Descriptions

Experiment Name	Experiment Description
CONTROL _{CCSM3}	Original fully coupled simulation conducted in support of IPCC AR4 (single-ensemble member)
CONTROL _{CLM3}	Off-line CLM3 forced with 6-hourly forcing from CONTROL _{CCSM3}
CONTROL	Same as CONTROL _{CLM3} but with CLM3.5 (revised hydrology)
SOILCARB	Same as CONTROL except with organic soil
SOILCARB_DS50	Same as SOILCARB except with ~50-m-deep soil column (five new layers)
SOILCARB_DS125	Same as SOILCARB except with ~125-m-deep soil column (seven new layers)

deep across much of the northern high latitudes [see, e.g., Zimov *et al.*, 2006]). Efforts are underway to develop a more realistic representation of the deep soil/rock column by compiling global data sets of soil depth and generalized bedrock type (J. Kaplan, personal communication, 2007) that are appropriate for the large GCM grid cells. Additional work involves adapting the soil hydrology code to accommodate a variable soil depth with underlying fractured bedrock. The simplified setup used here assumes that the deep soil parameters are globally uniform and fixed. The thermal conductivity for the frozen deep layers under this setup are $\sim 3.0 \text{ W m}^{-1} \text{ K}^{-1}$, which is comparable to that reported for saturated granitic rock [Clauser and Huenges, 1995]. There are many types of rock, of course, with reported rock thermal conductivities ranging from around $1.5 \text{ W m}^{-1} \text{ K}^{-1}$ for sedimentary rock up to $\sim 6 \text{ W m}^{-1} \text{ K}^{-1}$ for metamorphic rock [Clauser and Huenges, 1995], but the model is comparatively insensitive to the specification of the deep soil thermal properties. We tested the model for a range of assumed deep soil thermal conductivities (2.0 to $4.0 \text{ W m}^{-1} \text{ K}^{-1}$, representing various types of rock) and find that simply including versus omitting the deep soil layers (e.g., including or omitting the deep ground heat sink) has a far bigger impact on the soil temperature simulations than the specification of the deep soil properties.

[16] We also assessed how soil temperature initial conditions might impact results for experiments with a deep soil column by conducting tests with warm ($+2^\circ\text{C}$), cool (-2°C), and cold ($\sim 10^\circ\text{C}$) initial conditions. The impact of the soil temperature initial conditions on the equilibrium (e.g., spun-up) soil temperature is minimal.

[17] Although we conducted single point tests for a variety of soil depths, full experiments were conducted for only the 50 (five additional layers) and 125-m-deep (seven additional layers) columns. Henceforth, experiments with versions of CLM that include soil carbon and a deeper soil column are denoted SOILCARB_DS50 and SOILCARB_DS125 for the 50 and 125 m experiments, respectively. Table 1 lists the model configuration and labels for all the experiments included in this study.

3. Results

3.1. Soil Temperature Annual Cycle

[18] Although there are significant challenges when it comes to validating a model's soil temperature because of the high sensitivity of simulated and observed soil temperature to soil texture, moisture conditions, and snow cover in addition to the limitations imposed by relatively sparse measurements, the results from the new model appear to be more realistic than those of the previous model. Nicolsky *et al.* [2007] show that taking into account soil organic

material and deepening the soil column improves the annual cycle of soil temperature, particularly the summer maximum temperature, at a site near Deadhorse in the Alaskan Arctic. As expected, similar improvements are seen when we compare soil temperatures from off-line simulations forced with an observed historical data set [Qian *et al.*, 2006] to data from an array of Russian soil temperature monitoring sites that span most of Siberia [Zhang *et al.*, 2001]. Figure 2 shows annual cycle-depth temperature plots for CONTROL, SOILCARB, and SOILCARB_DS50 compared to observed annual cycle-depth temperatures. The broad qualitative improvements in the simulation are immediately apparent. The active layer thickness (ALT), defined as the depth to which the soil thaws each summer, is much shallower in SOILCARB and SOILCARB_DS50 than in CONTROL and its depth is in much closer agreement with observations. Soil temperatures below the active layer are also improved, especially in SOILCARB_DS50, where the removal of the zero flux boundary at 3.5 m results in smaller and more realistic seasonal temperature variations at depths below 2 m.

[19] Figure 3 shows the average simulated active layer thickness for the period 1970-1990 for CONTROL, SOILCARB, and SOILCARB_DS50. CONTROL_{CCSM3} and CONTROL_{CLM3} are qualitatively similar to CONTROL (not shown); SOILCARB_DS125 is qualitatively similar to SOILCARB_DS50 (not shown). The colder soil climate in SOILCARB contributes to an expansion of the diagnosed near-surface permafrost area. As seen in Figure 2, ALTs are considerably shallower in most regions. In experiments with a deeper soil column bottom boundary, near-surface permafrost extent is modestly larger and ALTs are slightly shallower.

[20] The total area containing near-surface permafrost (poleward of 45°N) is listed for all experiments in Table 2. For the period 1970-1989, the area in the original coupled simulation is $9.5 \times 10^6 \text{ km}^2$ (note that this is lower than the value of $10.5 \times 10^6 \text{ km}^2$ reported by Lawrence and Slater [2005] because it includes only land area north of 45°N and represents only a single ensemble member, whereas Lawrence and Slater [2005] reported the five-member ensemble average areal extent). The area in CONTROL_{CLM3} is a bit lower at $9.0 \times 10^6 \text{ km}^2$, reflecting the biases related to the experimental design that are discussed in section 2.2.

[21] Soil temperatures are slightly warmer in CLM3.5 (CONTROL) compared to CLM3 (CONTROL_{CLM3}), as noted in section 2.3, which results in an even lower diagnosed area containing near-surface permafrost ($8.5 \times 10^6 \text{ km}^2$). When compared to observed estimates for the area of continuous permafrost (90-100% coverage) and discontinuous permafrost (50-90% coverage) combined

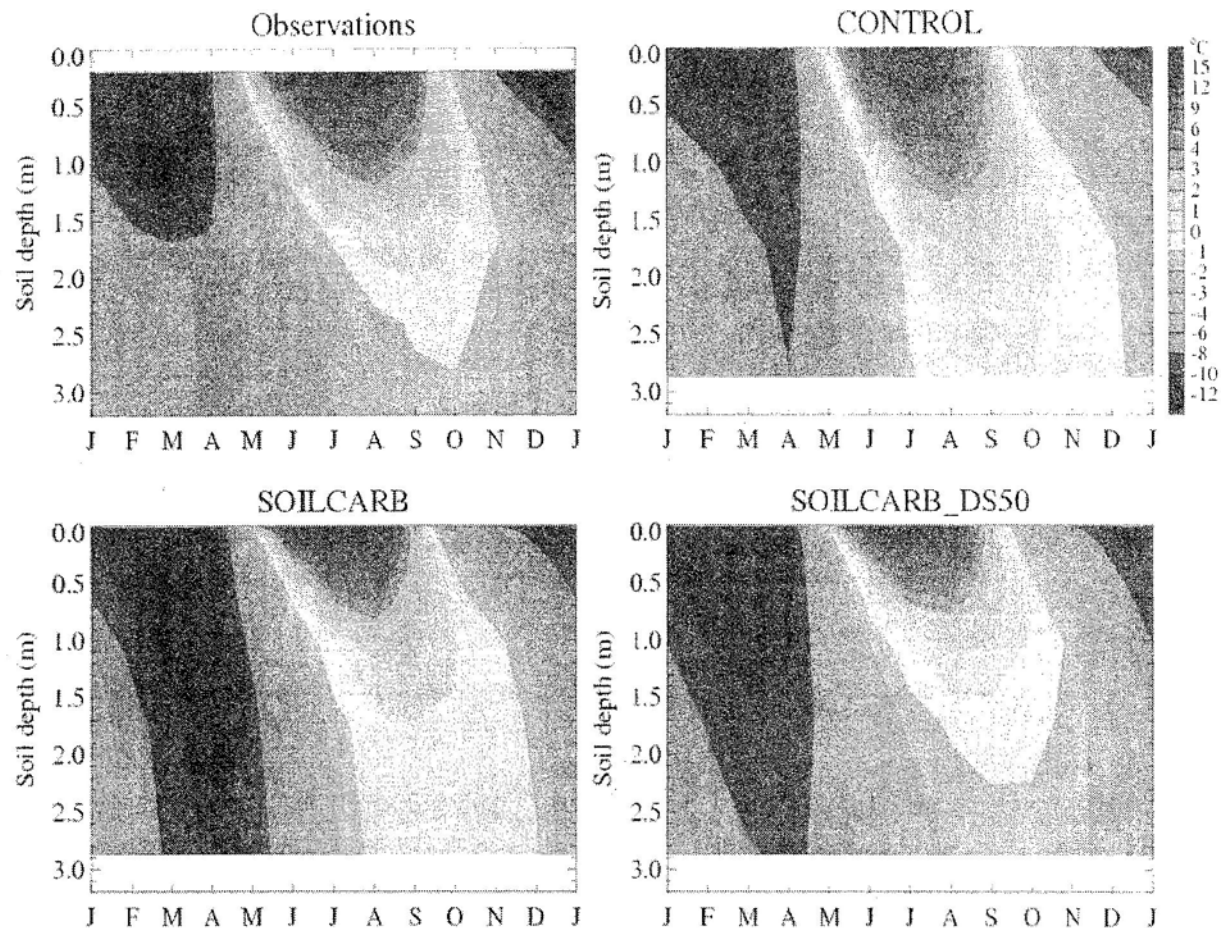


Figure 2. Annual cycle-depth plots of soil temperature averaged for selected stations in Russian soil temperature data set [Zhang *et al.*, 2001]. Stations include those that exhibit perennially frozen soil in top 3 m. Equivalent locations extracted and averaged over the same time period from off-line CLM simulations forced with observed data [Qian *et al.*, 2006].

(11.2–13.5 $\times 10^6$ km² for the equivalent region poleward of 45°N [Zhang *et al.*, 2000]), the total area simulated in CONTROL is clearly biased low. In the organic soil and deeper soil column experiments, the area with near-surface permafrost increases to 10.5 and 10.7 $\times 10^6$ km², respectively. These values compare reasonably with the observed permafrost extent, especially when one considers that the off-line experiments appear to be biased low by $\sim 0.5 \times 10^6$ km² compared to the coupled simulation. It is worth noting here that each grid box is represented by a single soil column. This prevents the explicit simulation of the sporadic or isolated permafrost classes which are typically found at the southern margins of the discontinuous permafrost boundary.

[22] It should be stressed that all the off-line CLM simulations are forced with data from the atmospheric component of CCSM3 obtained from a prior integration of the coupled model rather than a data set compiled from observations. The CCSM3 climate contains biases in temperature (Figure 4) when compared to observations, which will affect soil temperatures and permafrost extent. The southern portion of Alaska exhibits a cold bias in annual

mean air temperature while the region around the Ob River delta and east Siberian Plateau (70°N, 90°E) shows a warm bias; there are corresponding discrepancies between observed and modeled permafrost in these locations (Figure 3). Fortunately, annual mean air temperatures in the Arctic are not systematically biased warm or cold and, overall, the annual mean temperatures are reasonably well simulated in CCSM3. Nonetheless, there is room for improvement, especially since the reasonable simulations of annual mean temperatures mask more significant seasonal biases which include warmer winters and cooler summers than observed across much of the high latitudes. Snow depth and snow cover also affect soil temperatures and although CCSM3 snow simulation is reasonable in terms of its annual cycle and geographic extent, midwinter snow depths are biased systematically high by up to 40 cm when compared to climatological USAF snow depth data [Foster and Davy, 1988]. The simulated soil temperatures will reflect these biases in air temperature and snow depth. Reduction of the seasonal air temperature and snow depth biases is presently an area of focus for the CCSM development community.

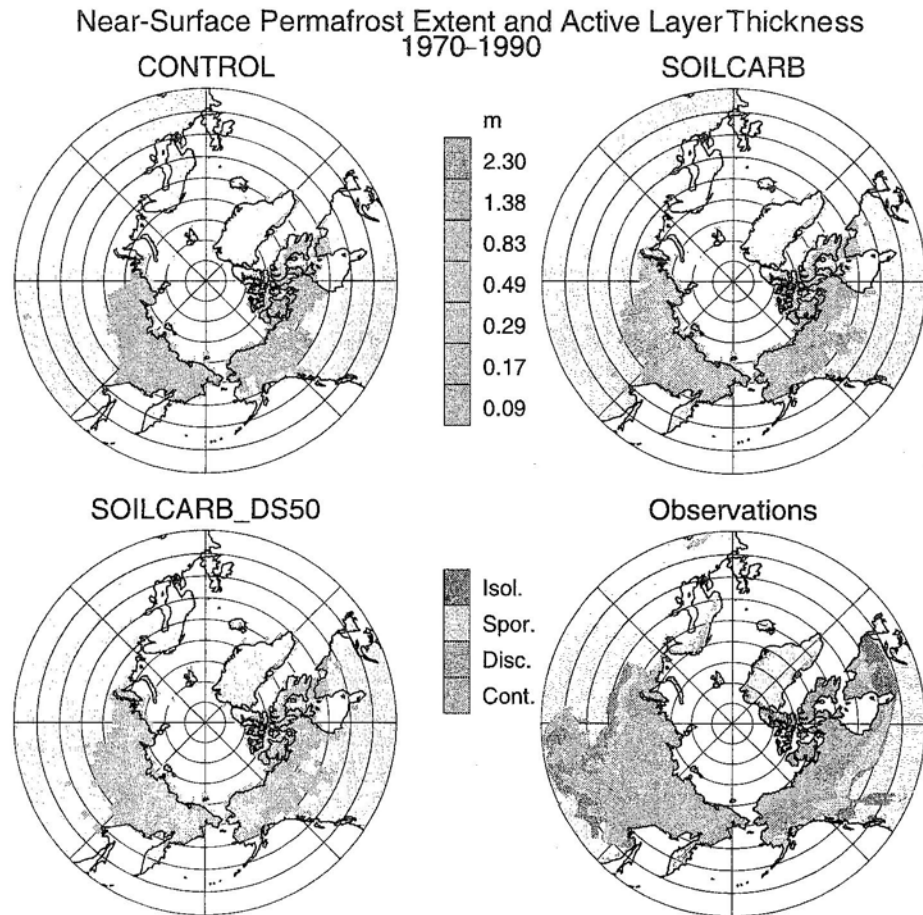


Figure 3. Modeled near-surface permafrost extent and ALT for off-line experiments CONTROL, SOILCARB, and SOILCARB_DS50 averaged over the period 1970–1990. Yellow denotes area where the dominant land unit in the CLM surface data set is glacier. Also shown are observed estimates of permafrost extent (continuous, discontinuous, sporadic, and isolated).

3.2. Trends in Near-Surface Permafrost Extent

[23] Time series of near-surface permafrost extent are shown in Figure 5 for the CONTROL, SOILCARB, SOILCARB_DS50, and SOILCARB_DS125 experiments. CONTROL_{CCSM3} and CONTROL_{CLM3} are not shown for the sake of clarity, but lie roughly in between the curves for CONTROL and SOILCARB. As noted above, experiments where soil organic matter is included are substantially cooler and near-surface permafrost extent is correspondingly broader (Table 2 and Figure 5). The rate of near-surface permafrost extent contraction is slower between 1990 and 2040 in SOILCARB ($87,000 \text{ km}^2 \text{ a}^{-1}$ in SOILCARB versus $111,000 \text{ km}^2 \text{ a}^{-1}$ in CONTROL). In simulations with a deeper soil column, the average rate of loss decreases further to $81,000$ and $76,000 \text{ km}^2 \text{ a}^{-1}$ (1990–2040) in SOILCARB_DS50 and SOILCARB_DS125. However, even though near-surface permafrost degrades at a slower rate in the latter three experiments, the total degradation by 2100 is almost as extensive as that seen in CONTROL.

[14] Although much of the simulated near-surface permafrost degrades in all experiments, it should be stressed that this does not mean that all permafrost disappears. As noted above, each grid box is represented by a single soil column,

which means that sporadic and isolated permafrost cannot be explicitly detected in the model. For regions where the maximum soil temperature rises above 0°C , but only marginally, it can be assumed that sporadic or isolated patches of permafrost would still be present in the warmer climate. In the deep soil experiments most of the permafrost found deeper in the soil column remains. Figure 6 shows a map that indicates the geographical extent of "deep" permafrost, here taken to be permafrost found between 10 and 30 m depth, for the SOILCARB_DS50 experiment for

Table 2. Total Area Containing Near-Surface Permafrost ($\times 10^6 \text{ km}^2$), or Total Area Containing Permafrost in the Case of the Observed Estimate, for Selected Periods^a

Experiment	1900–1919	1970–1989	2040–2059	2080–2099
Observed estimate	...	11.2–13.5
CONTROL _{CCSM3}	11.3	9.5	3.0	1.6
CONTROL _{CLM3}	11.0	9.0	2.5	1.4
CONTROL	10.2	8.5	1.8	0.9
SOILCARB	12.4	10.5	4.1	1.4
SOILCARB_DS50	12.7	10.7	4.6	1.5
SOILCARB_DS125	12.7	10.7	5.1	1.8

^aOnly area north of 45°N and nonglacier area included in calculation.

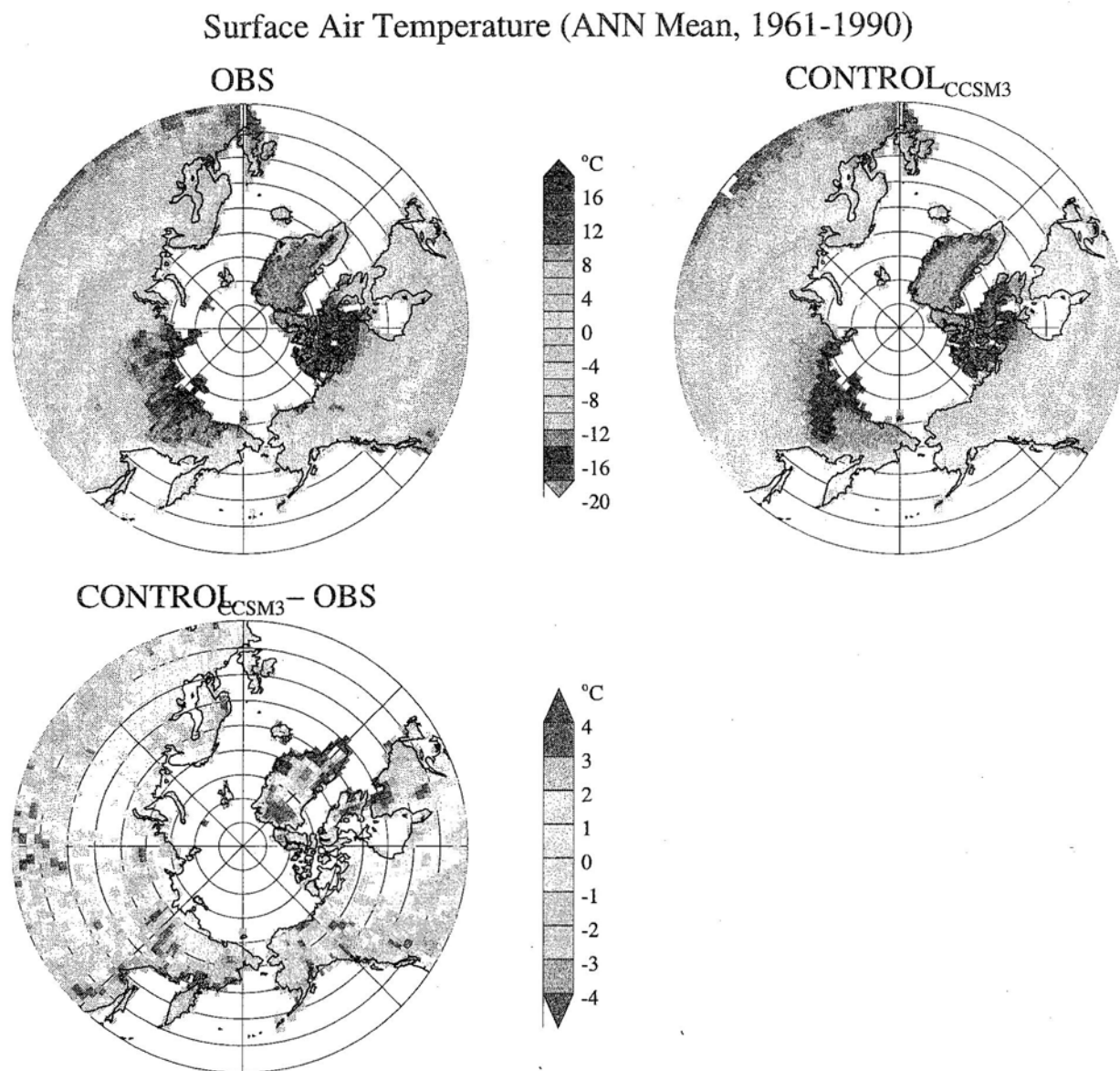


Figure 4. Annual mean surface air temperature for CONTROL_{CCSM3}, observations from C. J. Willmott and K. Matsuura (Terrestrial air temperature and precipitation: Monthly and annual climatologies, 2000, available online at <http://climate.geog.udel.edu/~climate>), and the difference between model and observations.

the periods 1970-1989 and 2080-2099. Over the course of the 21st century, a relatively small amount of deep permafrost degrades; this degradation occurs primarily at the southern edge of the simulated permafrost boundary. Over vast regions of Siberia and North America, deep permafrost remains intact at the end of the 21st century.

[25] The similarity of the time series of near-surface permafrost extent (Figure 5) for SOILCARB and the two deep soil experiments raises a question. Why is the rate of near-surface permafrost loss not strongly affected by the inclusion of the deep thermal reservoir associated with the new soil layers? Figure 7 shows time series of annual mean, annual maximum and annual minimum soil temperature at 1 m depth for SOILCARB and SOILCARB_DS50 averaged

over the Russian Arctic. The rises in annual mean soil temperature in the two experiments largely parallel each other and only diverge after the year 2000, but even then the difference is only marginal. Since the two versions of the model are driven with exactly the same temperature, precipitation, and radiative forcing, one would expect a priori that the thermal inertia of the deep soil layers would curtail soil temperature warming in SOILCARB_DS50. A possible explanation for this nonintuitive result is presented in Figure 8. Here, we plot time series of the change in ground heat flux and soil heat content for the same Russian Arctic region shown in Figure 7. Soil heat content in SOILCARB_DS50 is divided into the upper (0-3.5m) and lower (3.5-50m) portions of the soil. The change in

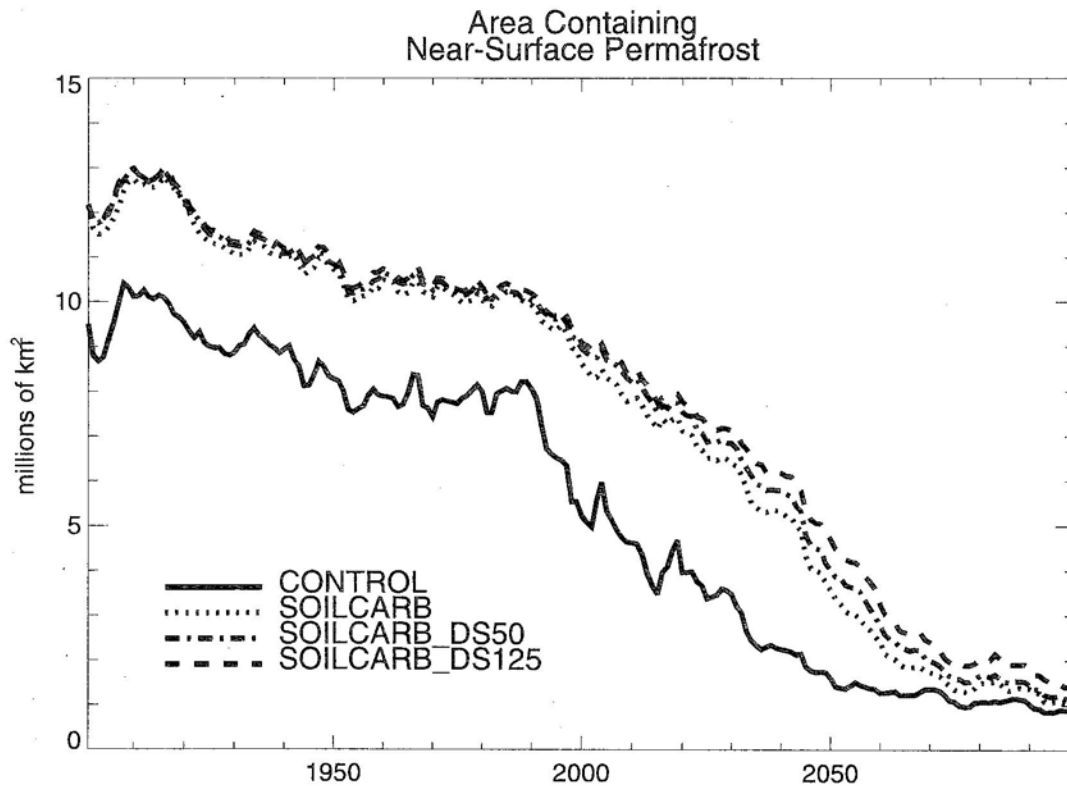


Figure 5. Time series of total area containing near-surface permafrost (north of 45°N and excluding ground underneath glaciers) for selected experiments.

annual mean ground heat flux, driven by changes in radiative forcing and surface air temperature, is small and roughly equivalent in the two experiments up until 1990. Over that period, soil heat content remains fairly constant as, overall, heat is neither being gained nor lost by the soil. After 1990, however, the ground heat flux time series for SOILCARB and SOILCARB_DS50 begin to diverge with the deep soil experiment absorbing significantly more energy. Soil heat content in the upper portion of the soil increases at essentially the same rate in both experiments, while the extra energy absorbed in SOILCARB_DS50 appears to accumulate at depth.

[26] So what is driving the difference in ground heat flux change? One possibility is that it is due to differences in the soil thermal gradient near the surface. A steeper thermal gradient induces stronger ground heat flux into the soil in summer and out of the soil in winter. Figure 8 (right) show the difference (SOILCARB_DS50 minus SOILCARB) in the vertical soil temperature gradient between the surface and 0.25 m depth across the annual cycle. Averages for three periods are shown: 1900–1919 when SOILCARB_DS50 is losing more heat than SOILCARB; 1970–1989 when annual ground heat flux in both models is near zero; and 2080–2099 when SOILCARB_DS50 is absorbing substantially more energy than SOILCARB. During the period 1900–1919, the soil in both models is losing energy in response to the relatively cool climate simulated by the coupled model. The thermal gradient of the upper soil during summer is steeper in SOILCARB, leading to a comparatively greater heat flux into the soil, which

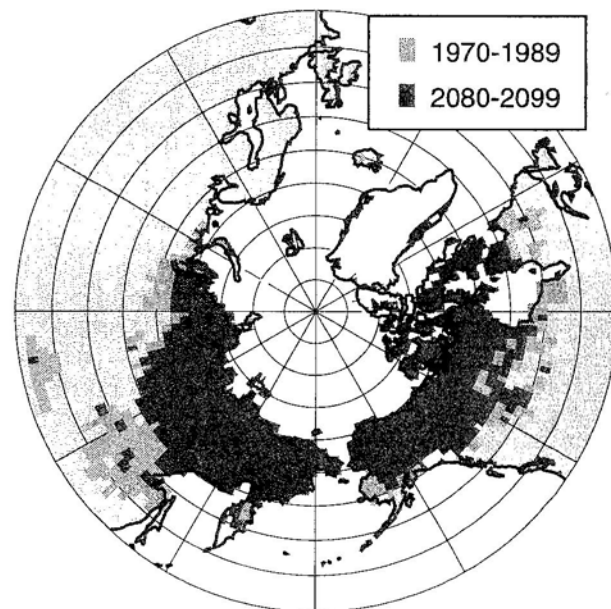


Figure 6. Simulated extent of deep permafrost at end of 20th and 21st centuries. Deep permafrost defined here as perennially frozen ground at depths between 10 and 30 m. Grid boxes with extensive glacier cover are masked out in a light gray color.

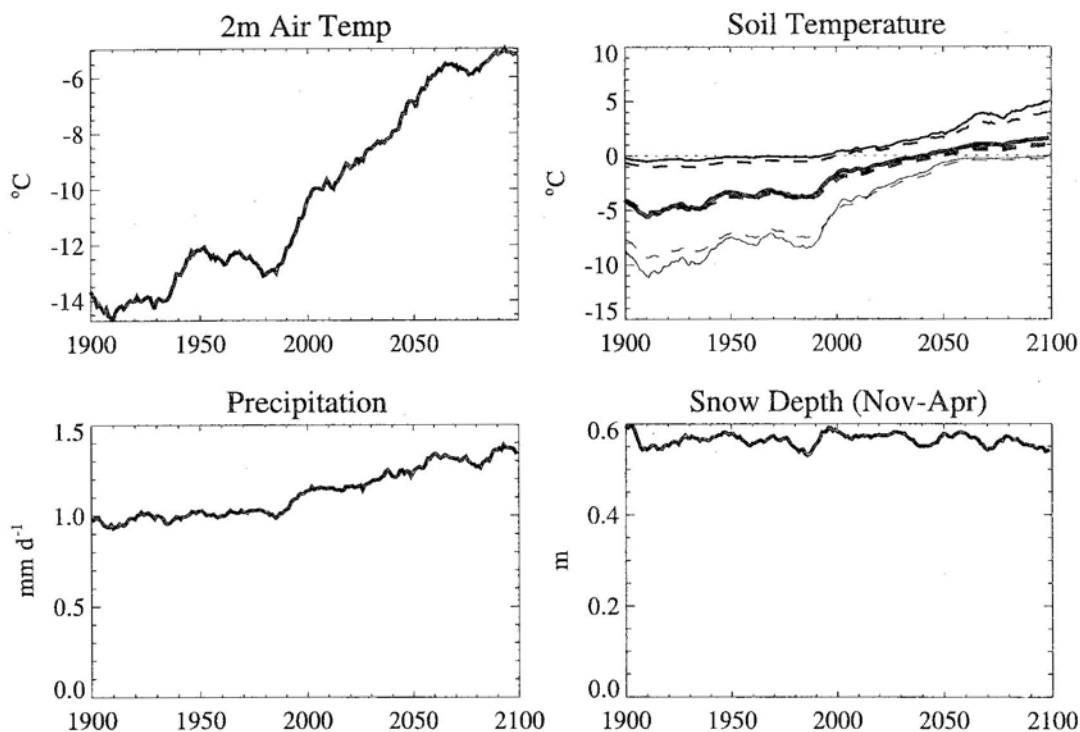


Figure 7. Time series of 2 m air temperature, 1 m soil temperature, precipitation, and snow depth (November–April mean) for area encompassing Russian Arctic (66.5–80°N, 70–170°E). For soil temperature, solid line is SOILCARB, and dashed line is SOILCARB_DS50. Line thicknesses for soil temperature are as follows: annual mean is the thick line, annual maximum is the medium line, and annual minimum is the thin line. The off-line SOILCARB and SOILCARB_DS50 exhibit almost identical simulated 2 m air temperature and snow depths and are forced with identical precipitation time series. All time series are smoothed with an 11-year running average.

corresponds during this time period to a reduced loss of energy relative to SOILCARB_DS50. In contrast, during the period 2080–2099, the thermal gradient is much steeper in SOILCARB_DS50, which leads to a comparatively larger increase in ground heat flux in response to warming air temperatures. It is possible that differences in the amplitude of the ground heat flux increase may be larger in off-line experiments than they would be in coupled experiments. In coupled simulations, an increase in ground heat flux would translate to reduced available energy at the surface which could potentially mitigate some surface warming. This result suggests that there may be added value in diagnosing future permafrost change as an integral part of the coupled climate system rather than modeling permafrost off-line as an external component forced with projected temperature changes.

4. Discussion

[17] The main result of this paper is that even with an improved land-surface scheme with explicit treatment of two important factors for permafrost dynamics, namely, accounting for the insulative properties of organic soil and the thermal inertia provided by cold deep ground, near-surface permafrost degrades sharply during the 21st century under the strong projected Arctic warming. The question remains as to how plausible these projections are. In this section, we

consider the results in the context of other modeling studies and review some potential sources of uncertainty which include biases in the simulated climate, the lack of a treatment of excess soil ice, and the potential roles that spin-up, vertical resolution, and coupling to the atmosphere could have on the projections of permafrost degradation.

4.1. Other Model Projections

[28] Prior assessments of likely changes to permafrost conditions vary considerably, although virtually all of them indicate that a significant amount of permafrost degradation will occur if the Arctic continues to warm [Anisimov and Nelson, 1997; Stendel and Christensen, 2002; Zhang et al., 2003; Sazonova et al., 2004; Sushama et al., 2006; Delisle, 2007; Saito et al., 2007; Zhang et al., 2008]. However, as discussed by Lawrence and Slater [2006], in modeling studies that are forced with 21st century temperature changes that are of the magnitude predicted in CCSM3 ($\sim 7.5^{\circ}\text{C}$ from 1900 to 2100), roughly equivalent changes to ALT are seen. For example, Anisimov and Poliakov [2003, Figure 2] model thaw depth deepening from depths of 0.4–3.0 m to 2.5–14 m under an 8°C warming over 100 years. Buteau et al. [2004] find downward thawing rates of up to 13 cm a^{-1} in ice rich permafrost for a 5°C warming over 100 years. More recently, Zhang et al. [2006] modeled the spatiotemporal changes in Canadian permafrost over the period 1850–2002 and into the future. Their 63-layer,

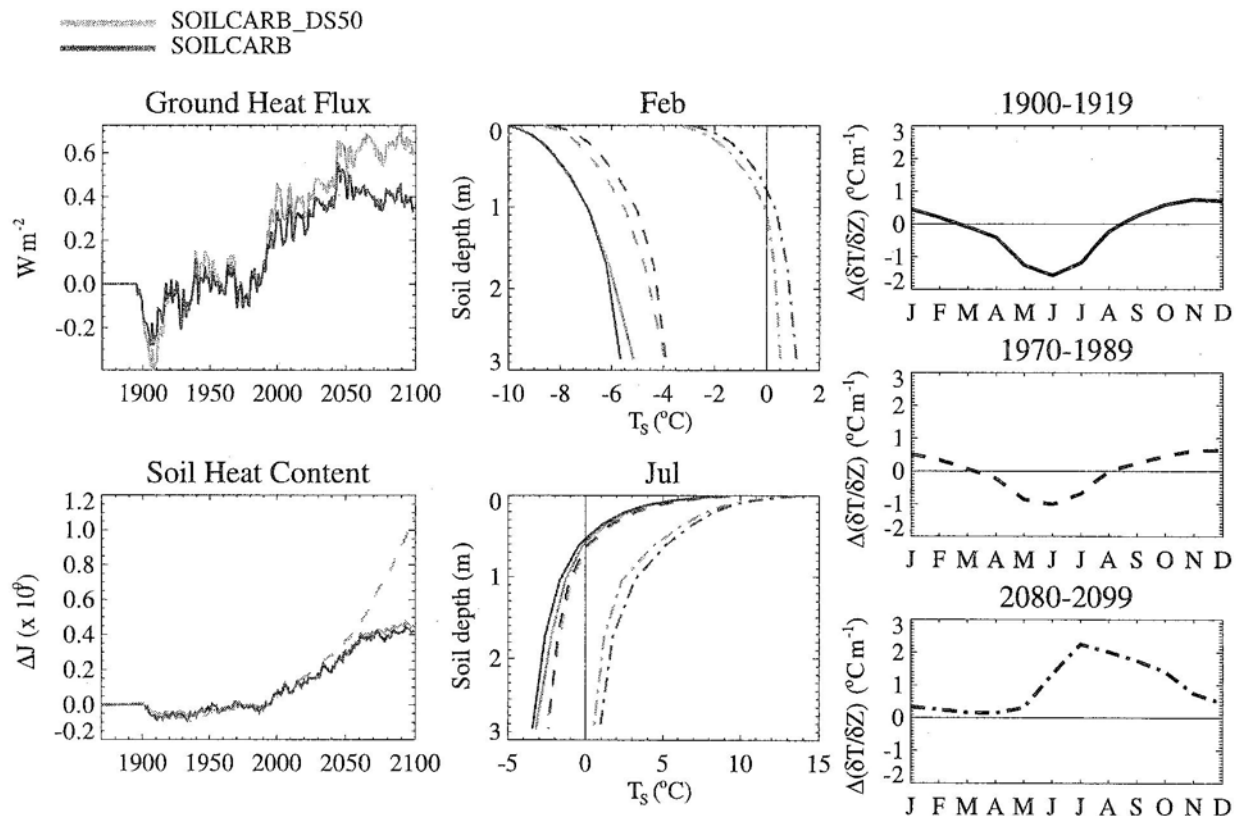


Figure 8. (left) Time series of annual ground heat flux and change in soil heat content for SOILCARB and SOILCARB_DS50 averaged over the Russian Arctic (66.5–80°N, 70–170°E). For soil heat content, solid lines are soil heat content change in the upper 3.5 m, and dashed line is change in soil heat content for 3.5–50 m. (middle) Temperature-depth profiles for February and July averaged over the same region for 1900–1919 (solid line), 1970–1989 (dashed line), 2080–2099 (dashed-dotted line). (right) Annual cycle of difference in soil thermal gradient near the soil surface (surface minus ~25 cm) for SOILCARB_DS50 – SOILCARB.

120-m-deep model is process oriented, like CLM, and includes snow and soil moisture dynamics, organic soil and excess soil ice. Over the persistent permafrost region of Canada, they see the mean depth to the permafrost table increasing from ~0.65 m 1850 to over 1.2 m in 2002, with the rate of deepening accelerating over the last 15–20 years. In a follow up paper projecting from 1990 to 2100, the persistent permafrost region shows a change in mean depth to the permafrost table from 1 m to over 6 m with a temperature forcing similar to that simulated in CCSM [Zhang *et al.*, 2008]. Simulations with the Terrestrial Ecosystem Model coupled to a deep soil thermal model and forced with a similar amplitude of warming (~+6.4°C from 2000–2010 to 2090–2100, 60–90°N) show a similar decrease in near-surface permafrost extent (defined in that paper as permanently frozen ground in top 2m of soil) of 8×10^6 km² [Euskirchen *et al.*, 2006], although that model simulates a larger present-day permafrost extent, in better agreement with observations. Last, a recent analysis of data from the high-resolution MIROC coupled GCM reveals a projected 60% contraction of the area containing near-surface permafrost by 2100 [Saito *et al.*, 2007], which is less than that simulated in CCSM3, but still indicates a large-scale degradation of near-surface permafrost.

4.2. Biases in the Simulated Climate

[29] It is important to consider the role of biases in the simulated climate. Nicolsky *et al.* [2007] conclude that, given accurate forcing, CLM with modifications similar to those described here, can reasonably simulate soil temperatures in the upper 3m of the soil. The phrase, given the correct forcing, is relevant. Annual mean temperature biases in CCSM3, for this simulation at least, are not unreasonable and more importantly are not systematically warm or cool. However, there are systematic biases in annual temperature range (too low) and snow depth (too high) that could result in warmer soil conditions at the end of the 20th century than are observed in nature. The extent and the timing of near-surface permafrost degradation are almost certainly sensitive to these biases. Reduction of Arctic temperature and snow biases remains an area of focus for developers of CCSM.

4.3. Other Model Limitations (Excess Soil Ice, Vegetation Feedbacks, Greenhouse Gas Feedbacks)

[30] There are other issues to consider as well. At the present time, CLM does not simulate or account for excess soil ice, pockets of ice that are commonly found in permafrost ground that are present in excess of the available soil

pore space [Zhang *et al.*, 2000]. Under the present CLM architecture, it is not possible to explicitly model excess soil ice, although potential solutions are currently being explored. On average, ice content in SOILCARB_DS50 is 15–20% higher than in SOILCARB because of SOILCARB_DS50's colder temperatures below the active layer. The increased ice content beneath the active layer restricts the movement of water and limits summer drainage. Even with the higher ice content, the magnitude of the Arctic warming is enough to melt this extra ice by the end of the 21st century for most locations.

[31] Changes in vegetation cover can also affect the evolution of soil temperatures. After initial permafrost degradation due to warming, biological processes including sedge growth and subsequent peat formation can provide a negative feedback that limits the vertical extent of degradation [Jorgenson *et al.*, 2001, 2006]. The expansion of shrubs across the Arctic tundra can lead to increased winter snow depth (warmer soil temperatures) and earlier snowmelt (warmer soil temperatures) while also providing more summer shading of the ground surface (cooler soil temperatures) [Sturm *et al.*, 2001, 2005]. At present, these types of ecological processes are not simulated in CLM. Future model development efforts will focus on representing such processes, for example by incorporating a shrub vegetation type into the CLM-Dynamic Global Vegetation Model [Levis *et al.*, 2004].

[32] Last, warming and thawing may lead to enhanced decomposition of soil organic matter which could conceivably result in vast quantities of carbon dioxide (and/or methane if wetland areas and functioning change) being released to the atmosphere [Zimov *et al.*, 2006]. The release of these greenhouse gases could amplify climate warming and thereby indirectly increase the rate of permafrost degradation.

4.4. Soil Column Depth, Spin-Up, and Vertical Resolution

[33] One question that is raised by this study is what soil column depth is appropriate and required for use in a GCM land-surface scheme. Alexeev *et al.* [2007] argue that the deeper the soil column the better, especially for longer-timescale applications. Molders and Romanovsky [2006] note that the soil column depth should exceed the depth of seasonal changes in soil temperature and moisture states, which can be as deep as 15–20 m [Romanovsky and Osterkamp, 1997]. Both the 50 and 125 m columns meet this criterion. For the climate-change simulations conducted here, the depth of the column (e.g., 50 or 125 m) does not have a strong influence on the results. Soil temperature rise in soil layers near the surface is only marginally slower in SOILCARB_DSI25 compared to SOILCARB_DS50 and in most locations near-surface soil temperatures are nearly indistinguishable by 2100 (not shown). Further, any potential benefits that may be derived from a very deep soil column need to be balanced by considerations of computational efficiency. In addition to the added computational expense of a 17-layer model compared to a 15-layer model, the deeper the soil column the longer the spin-up timescale for the deep soil layers. The time to equilibrium for soil layer 15 (midpoints at approximately 35 m depth) is nearly twice as long for the 125-m-deep model compared to the

50-m-deep model. In either case, some forms of accelerated spin-up of deep soil temperatures may be required as small trends in deep soil heat content can be found even after 400 years for locations where the mean climate hovers near the freezing level. Taking these considerations into account and also considering the small amplitude of potential soil temperature errors for the shallower model in the context of the likely much larger climate temperature bias errors, it is reasonable to conclude that the 15-layer, ~50-m-deep soil column would be sufficient for climate change simulations.

[34] A similar question to that of soil column depth can be asked with respect to the soil model vertical resolution. Does the highly discretized nature of the 15-layer soil model affect the transient simulation? To address this, we tested a 30-layer version of the model and found that, although the higher-resolution model better resolves the active layer thickness as expected, increasing the vertical resolution has a minimal impact on soil temperature trends. That is, for equivalent soil depths soil temperatures rise and permafrost thaws at roughly the same rate over the 21st century in both the low and high vertical resolution configurations. The argument then is as above for soil column depth that the computational expense incurred through increased vertical resolution does not appear to be warranted, at least in the context of climate change. For applications where more accurate knowledge of active layer depth is required, a higher-resolution model may be preferred.

[35] Two other issues with the model require mention. Small soil temperature errors that are generated through the use of the numerically efficient predictor-corrector method for soil water phase change could be a source of bias [Nicolsky *et al.*, 2007], although the small timestep used in the model (30 min) limits the amplitude of these biases. Additionally, heat advection associated with water infiltrating into and through the soil is not represented. This source of energy for the soil may be important, particularly during the snowmelt period when large volumes of water enter the soil column.

4.5. Two-Way Land-Atmosphere Interactions

[36] For the sake of computational efficiency and to permit clean comparisons across the different versions of CLM, the simulations completed for this study were conducted off-line. In general, however, it would be preferable where possible to complete coupled simulations so that the two-way interactions between changes in climate and the land surface can be captured. Lawrence and Slater [2007] find that CAM-CLM simulations with organic soil exhibit substantially warmer surface air temperature than the control simulations. The difference in air temperature is due to an intricate atmospheric feedback induced by a shift toward lower surface latent heat flux and greater sensible heat flux in the version with organic soil. There is also some suggestion from the results shown here, although indirect, that two-way land-atmosphere interactions may be important when a deep soil column is included. As noted above, more energy is absorbed by the land under warming in the deep soil experiments due, apparently, to a steeper near-surface soil temperature gradient. Additionally, it is important to note that a deeper soil column means that the potential for the land to store heat is greatly enhanced, as discussed by Stevens *et al.* [2007]. Errors in subsurface heat

accumulation when a shallow column is used can be more than 1 order of magnitude greater than the estimated heat absorbed by continental areas over the last 50 years [Beltrami *et al.*, 2006; Stevens *et al.*, 2007]. It is possible that in a coupled simulation, the stronger increase in ground heat flux would contribute to reduced available energy at the surface and associated reductions in surface warming and permafrost degradation. Consequently, where possible, future simulations will be done in a coupled framework.

5. Summary

[37] Results presented by Lawrence and Slater [2005] indicate that the strong Arctic warming predicted in CCSM3 drives severe degradation of near-surface permafrost during the 21st century. These projections are recalculated with an improved version of CLM3 that explicitly accounts for the physical and hydrologic properties of soil organic matter and with a soil column depth extended to 50 or 125 m. Soil temperature dynamics, when forced with observed climate forcing, are much improved in the new version of the model. More realistic active layer thicknesses and, more generally, improved seasonal soil temperature cycles throughout the upper portion of the soil column are seen. When forced off-line with archived atmospheric data from a fully coupled CCSM3 simulation of the climate of the 20th century, the colder ground climate in the revised version of CLM results in a near-surface permafrost extent ($10.7 \times 10^6 \text{ km}^2$, for the area north of 45°N) that is improved over the standard model ($1 \times 10^6 \text{ km}^2$). These values compare reasonably, although they are still biased low, with observed estimates for the total area of continuous and discontinuous permafrost ($11.2\text{--}13.5 \times 10^6 \text{ km}^2$). Since the revised land model reasonably simulates soil temperatures and their annual cycle when forced with observed data (Figure 2), it is reasonable to infer that the remaining bias in permafrost area, which can be interpreted as a soil temperature bias, is due to biases in the simulated air temperature (annual range), snow depth or other aspects of the CCSM3 climate. However, a contribution to the bias due to missing physics, imperfectly parameterized processes in the land model, insufficient resolution in the vertical or horizontal dimensions, or inaccuracies in the surface and soil texture data sets employed cannot be discounted.

[38] The rate of near-surface permafrost degradation, in response to the strong Arctic warming ($\sim +7.5^\circ\text{C}$ over land, 1900–2100 simulated by CCSM3 under the SRES A1B greenhouse gas emissions scenario), is slower in the improved versions of CLM for the period 1990–2040 (111,000, 87,000, 81,000, and $76,000 \text{ km}^2 \text{ a}^{-1}$ in CONTROL, SOILCARB, SOILCARB_DS50, and SOILCARB_DS25, respectively). However, even though the rates of degradation are initially depressed, the strong Arctic warming is enough to substantially reduce the total area containing near-surface permafrost in CCSM3 by 2100. Permafrost degradation of this magnitude, if it occurs, is likely to invoke a number of hydrological, biogeochemical, and ecological feedbacks in the Arctic system.

[39] Interestingly, even though a priori one would expect that the cold deep soil layers would provide thermal inertia that would restrict warming of the near-surface soil, experiments with a deep soil column do not exhibit a substantively

slower rate of degradation compared to those with a shallow soil column. The lack of a strong difference is apparently due to a steeper near-surface vertical soil temperature gradient in the deep soil experiments which leads to enhanced absorption of the excess surface energy that is available because of warming. The extra absorbed energy accumulates at depth while the near-surface soil accumulates heat at roughly the same rate in deep soil column and shallow soil column experiments. Potential feedbacks on surface air temperature further support the need to analyze permafrost and permafrost change in coupled land-atmosphere models where possible.

[40] As noted in the Introduction, the broader scientific challenge is to increase our understanding and representation of the complex hydrological, biogeophysical, and biogeochemical feedbacks that are anticipated in the Arctic. Future work will focus on the continued development of the model physics and biogeophysics (e.g., dynamic wetlands, dynamic vegetation) that is required to better represent the impact of climate change on permafrost and the feedbacks of permafrost degradation on regional and global climate.

[41] **Acknowledgments.** This research was supported by the Office of Science (BER), U. S. Department of Energy, Cooperative Agreement DE-FC02-97ER62402. NCAR is supported by the National Science Foundation. Additional support comes from the National Science Foundation grants OPP-022-9769, OPP-022965-1, ARC-0632400, ARC-052058, and ARC-0612533 and IARC-NSF CA Project 3.1 Permafrost Research and NASA NNG04GJ39G and NNG06GH48G. We would like to thank the three anonymous reviewers for their constructive comments which substantially improved the quality of this paper.

References

- Alexeev, Y. A., D. J. Nicolsky, Y. E. Rornanovsky, and D. M. Lawrence (2007), An evaluation of deep soil configurations in the CLM3 for improved representation of permafrost, *Geophys. Res. Lett.*, **34**, L09502, doi:10.1029/2007GL029536.
- Anisimov, O. A., and F. E. Nelson (1997), Permafrost zonation and climate change in the Northern Hemisphere: Results from transient general circulation models, *Clim. Change*, **35**, 241–258, doi:10.1023/A:1005315409698.
- Anisimov, O. A., and V. Y. Poliakov (2003), GIS assessment of climate change impacts in permafrost regions, in *Permafrost: Proceedings of the International Conference on Permafrost*, vol. 1, edited by M. Phillips, S. M. Springman, and L. U. Arenson, pp. 9–14, A. A. Balkema, Lisse, Belgium.
- Beltrami, N., E. Bourlon, L. Kellman, and J. F. Gonzales-Ronco (2006), Spatial patterns of ground heat gain in the Northern Hemisphere, *Geophys. Res. Lett.*, **33**, L06717, doi:10.1029/2006GL025676.
- Bum, C. N., and F. E. Nelson (2006), Comment on "A projection of near-surface permafrost degradation during the 21st century", *Geophys. Res. Lett.*, **33**, L21503, doi:10.1029/2006GL02706.
- Buteau, S., R. Fortier, G. Delisle, and M. Allard (2004), Numerical simulation of the impacts of climate warming on a permafrost mound, *Pennacast Periglacial Processes*, **15**, 41–57, doi:10.1002/ppp.474.
- Chapin, F. S., III, et al. (2005), Role of land-surface changes in Arctic summer warming, *Science*, **310**, 657–660, doi:10.1126/science.1117368.
- Chapman, W. L., and J. E. Walsh (2007), Simulations of Arctic temperature and pressure by global coupled models, *J. Clim.*, **20**, 609–632, doi:10.1175/JCLI4026.1.
- Christensen, T. R., T. R. Johansson, H. J. Akerman, M. Mastepanov, N. Maimor, T. Friberg, P. Crill, and B. H. Svensson (2004), Thawing subarctic permafrost: Effects on vegetation and methane emissions, *Geophys. Res. Lett.*, **31**, L04501, doi:10.1029/2003GL018680.
- Clauser, C., and E. Huenges (1995), Thermal conductivity of rocks and minerals, in *Rock Physics and Phase Relations: A Handbook of Physical Constants*, edited by T. J. Ahrens, pp. 105–126, AGU, Washington, D.C.
- Collins, W. D., et al. (2006), The Community Climate System Model Version 3 (CCSM3), *J. Clim.*, **19**, 2122–2143, doi:10.1175/JCLI3761.1.
- Delisle, G. (2007), Near-surface permafrost degradation - how severe during the 21st century?, *Geophys. Res. Lett.*, **34**, L09503, doi:10.1029/2007GL029323.

- Euskirchen, E. S., et al. (2006), Importance of recent shifts in soil thermal dynamics on growing season length, productivity, and carbon sequestration in terrestrial high-latitude ecosystems, *Globed Change Biol.*, **12**, 731–750, doi: 10.1111/j.1365-2486.2006.01113.x.
- Foster, D. F., Jr., and R. D. Davy (1988), Global snow depth climatology, *U. S. Air Force Tech. Note USAFETAC/TN-88/006*, Scott Air Force Base, St. Louis, Ill.
- Global Soil Data Task (2000), Global Gridded Surfaces Of Selected Soil Characteristics (IGBP-DIS), <http://www.daac.orn.gov/>, Oak Ridge Natl. Lab. DAAC, Oak Ridge, Tenn.
- Jorgenson, M. T., C. H. Racine, T. C. Walters, and T. E. Osterkamp (2001), Permafrost degradation and ecological changes associated with a warming climate in central Alaska, *Clim. Change*, **48**, 551–579, doi: 10.1023/A:1005667424292.
- Jorgenson, M. T., Y. L. Shur, and E. R. Pullman (2006), Abrupt increase in permafrost degradation in Arctic Alaska, *Geophys. Res. Lett.*, **25**, L02503, doi: 10.1029/2005GL024960.
- Lawrence, P. J., and T. N. Chase (2007), Representing a new MODIS consistent land surface in the Community Land Model (CLM3.0), *J. Geophys. Res.*, **112**, G01023, doi: 10.1029/2006JG000168.
- Lawrence, D. M., and A. G. Slater (2005), A projection of severe near-surface permafrost degradation during the 21st century, *Geophys. Res. Lett.*, **32**, L24401, doi: 10.1029/2005GL025080.
- Lawrence, D. M., and A. G. Slater (2006), Reply to comment by C.R. BURN and F.E. Nelson on "A projection of near-surface permafrost degradation during the 21st century", *Geophys. Res. Lett.*, **33**, L21504, doi: 10.1029/2006GL027955.
- Lawrence, D. M., and A. G. Slater (2007), Incorporating organic soil into a global climate model, *Dyn.*, doi:10.1007/s00382-007-0278-1.
- Lawrence, D. M., P. E. Thornton, K. W. Oleson, and G. B. Bonan (2007), Partitioning of evaporation into transpiration, soil evaporation, and canopy evaporation in a GCM: Impacts on land-atmosphere interaction, *J. Hydrometeorol.*, **8**, 862–880, doi:10.1175/JHM596.1.
- Levis, S., G. B. Bonan, M. Vertenstein, and K. W. Oleson (2004), The Community Land Model's dynamic global vegetation model (CLM-DGVM): Technical description and user's guide, *NCAR Tech. Note TN-459+IA*, 50 pp., Natl. Cent. for Atmos. Res., Boulder, Colo.
- McGuire, A. D., F. S. Chapin, J. E. Walsh, and C. Wirth (2006), Integrated regional changes in Arctic climate feedbacks: Implications for the Global Climate System, *Annu. Rev. Environ. Resour.*, **31**, 61–91, doi:10.1146/annurev.energy.31.020105.100253.
- Meehl, G. A., W. M. Washington, B. D. Santer, W. D. Collins, J. M. Arblaster, A. Hu, D. M. Lawrence, H. Teng, L. E. Buja, and W. G. Strand (2006), Climate change in the 20th and 21st centuries and climate change commitment in the CCSM3, *1. Clim.*, **19**, 2597–2616, doi:10.1175/JCLI3746.1.
- Molders, N., and V. E. Romanovsky (2006), Long-term evaluation of the Hydro-Thermodynamic Soil-Vegetation Scheme's frozen ground/permafrost component using observations at Barrow, Alaska, *J. Geophys. Res.*, **111**, D04105, doi: 10.1029/2005JD000597.
- Nicolsky, D. J., V. E. Romanovsky, V. A. Alexeev, and O. M. Lawrence (2007), Improved modeling of permafrost dynamics in a GCM land-surface scheme, *Geophys. Res. Lett.*, **34**, L08501, doi: 10.1029/2007GL029525.
- Niu, G. Y., and Z. L. Yang (2006), Effects of frozen soil on snowmelt runoff and soil water storage at a continental scale, *J. Hydrometeorol.*, **7**, 937–952, doi:10.1175/JHM538.1.
- Niu, G. Y., Z. L. Yang, R. E. Dickinson, L. E. Gulden, and H. Su (2007), Development of a simple groundwater model for use in climate models and evaluation with Gravity Recovery and Climate Experiment data, *J. Geophys. Res.*, **112**, D07103, doi: 10.1029/2006JD007522.
- Oleson, K. W. et al. (2004), Technical description of the Community Land Model (eLM), *NCAR Tech. Note TN-4M+STR*, 174 pp. Natl. Cent. for Atmos. Res., Boulder, Colo.
- Osterkamp, T. E. (2005), The recent warming of permafrost in Alaska, *Global Planet. Change*, **49**, 187–202, doi: 10.1016/j.gloplacha.2005.09.001.
- Osterkamp, T. E., and J. C. Jorgenson (2006), Warming of permafrost in the Arctic National Wildlife Refuge, Alaska, *Permafrost Periglacial Processes*, **17**, 65–69, doi: 10.1002/ppp.538.
- Osterkamp, T. E., and V. E. Romanovsky (1999), Evidence for warming and thawing of discontinuous permafrost in Alaska, *Permafrost Periglacial Processes*, **10**, 17–37, doi:10.1002/(SICI)1099-1530(199901)10:1<17::AID-PPP303>3.0.CO;2-4.
- Payette, S., A. Delwaide, M. Caccianiga, and M. Beauchemin (2004), Accelerated thawing of subarctic peatland permafrost over the last 50 years, *Geophys. Res. Lett.*, **31**, L18208, doi:10.1029/2004GL020358.
- Qian, T., A. Dai, K. E. Trenberth, and K. W. Oleson (2006), Simulation of global land surface conditions from 1948 to 2002: Part 1: Forcing data and evaluations, *J. Hydrometeorol.*, **7**, 953–975, doi: 10.1175/JHM540.1.
- Romanovsky, V. E., and T. E. Osterkamp (1997), Thawing of the active layer on the coastal plain of the Alaskan Arctic, *Permafrost Periglacial Processes*, **8**, 1–22, doi:10.1002/(SICI)1099-1530(199701)8:1<1::AID-PPP243>3.0.CO;2-U.
- Romanovsky, Y., M. Burgess, S. Smith, K. Yoshikawa, and I. Brown (2002), Permafrost temperature records: Indicators of climate change, *Eos Trans. AGU*, **83**(50), 589.
- Saito, K. M., Kimoto, T., Zhang, K., Takata, and S. Ernori (2007), Evaluating a high-resolution climate model: Simulated hydrothermal regimes in frozen ground regions and their change under the global warming scenario, *J. Geophys. Res.*, **112**, F02S11, doi: 10.1029/2006JF000577.
- Sazonova, T. S., V. E. Romanovsky, I. E. Walsh, and D. O. Sergueev (2004), Permafrost dynamics in the 20th and 21st centuries along the East Siberian transect, *J. Geophys. Res.*, **109**, D01108, doi: 10.1029/2003JD003680.
- Smerdon, J. E., and M. Stieglitz (2006), Simulating heat transport of harmonic temperature signals in the Earth's shallow subsurface: Lower-boundary sensitivities, *Geophys. Res. Lett.*, **33**, L14402, doi: 10.1029/2006GL026816.
- Smith, L. C., Y. Sheng, G. M. MacDonald, and I. D. Hinzman (2005), Disappearing Arctic lakes, *Science*, **308**, 1429, doi: 10.1126/science.1108142.
- Stendel, M., and J. H. Christensen (2002), Impact of global warming on permafrost conditions in a coupled GeM, *Geophys. Res. Lett.*, **29**(13), 1632, doi: 10.1029/2001GL014345.
- Stevens, M. B., J. E. Smerdon, I. F. Gonzalez-Ronco, M. Stieglitz, and H. Beltrami (2007), Effects of bottom boundary placement on subsurface heat storage: Implications for climate model simulations, *Geophys. Res. Lett.*, **34**, L02702, doi: 10.1029/2006GL028546.
- Sturm, M., J. P. McFadden, G. E. Liston, F. S. Chapin III, C. H. Racine, and J. Holmgren (2001), Arctic climate implications, *J. Clim.*, **14**, 336–344, doi: 10.1175/1520-0442(2001)014<0336:SSIA>2.0.CO;2.
- Sturm, M., J. Schimel, G. Michaelson, I. M. Welker, S. F. Oberbauer, G. E. Liston, J. Fahnestock, and Y. E. Romanovsky (2005), Winter biological processes could help convert arctic tundra to shrubland, *Bioscience*, **55**, 17–26, doi: 10.1641/0006-3568(2005)055/0017:WBPCHCJ/002.
- Sushama, L., R. Laprise, and M. Allard (2006), Modeled current and future soil thermal regime for northeast Canada, *J. Geophys. Res.*, **111**(D) 18111, doi: 10.1029/2005JD007027.
- Tape, K. M., Sturm, and C. Racine (2006), The evidence for shrub expansion in Northern Alaska and the Pan-Arctic, *Global Change Biol.*, **12**, 686–702, doi: 10.1111/j.1365-2486.2006.01128.x.
- Thornton, P. E., and N. Zimmerman (2007), An improved canopy integration scheme for a land surface model with prognostic canopy structure, *J. Clim.*, **20**, 3902–3923, doi:10.1175/JCLI14222.1.
- Zhang, T., J. A. Heginbottom, R. G. Ban, and J. Brown (1000), Further statistics on the distribution of permafrost and ground ice in the Northern Hemisphere, *Polar Geogr.*, **24**, 126–131.
- Zhang, T., R. Ban, D. Gilichinsky and compilers CWO1, Russian Historical Soil Temperature Data, <http://nsidc.org/data/arcs078.html>, Natl. Snow and Ice Data Cent., Boulder, Colo. (Updated 2006.)
- Zhang, Y., W. J. Chen, and J. Cihlar (2003), A process-based model for quantifying the impact of climate change on permafrost thermal regimes, *J. Geophys. Res.*, **108**(D22), 4695, doi: 10.1029/2002JD003354.
- Zhang, Y., W. J. Chen, and D. W. Riseborough (2006), Temporal and spatial changes of permafrost in Canada since the end of the Little Ice Age, *J. Geophys. Res.*, **111**, D22103, doi: 10.1029/2006JD007284.
- Zhang, Y., W. J. Chen, and D. W. Riseborough (2008), Transient projections of permafrost distribution in Canada during the 21st century under scenarios of climate change, *Global Planet. Change*, **60**, 443–456, doi: 10.1016/j.gloplacha.2007.05.003.
- Zimov, S. A., E. A. G. Schuur, and F. S. Chapin (2006), Permafrost and the global carbon budget, *Science*, **312**, 1612–1613, doi:10.1126/science.1128908.

D. M. Lawrence, Climate and Global Dynamics Division, National Center for Atmospheric Research, P.O. Box 3000, Boulder, CO 80307, USA. (dlawren@ucar.edu)

D. J. Nicolsky and Y. E. Romanovsky, Geophysical Institute, University of Alaska Fairbanks, 903 Koyukuk Drive, Fairbanks, AK 99775, USA.

A. G. Slater, Cooperative Institute for Research in Environmental Sciences, University of Colorado, 216 UBC, Boulder, CO 80309, USA.